Dentith et al., present the implementation of oceanic stable carbon isotope (^{13}C) in the ocean component of the FAMOUS model. The model includes carbon fractionation during air-sea gas exchange, and photosynthesis. Three schemes are tested for fractionation during photosynthesis, with the more complex schemes not improving the model-data comparison. The oceanic $\delta^{13}C$ values are globally higher in the model than in observations, probably due to the representation of both the oceanic circulation and marine carbon cycle in the model. I agree with the conclusions of the authors that the model should probably be re-tuned for both its oceanic circulation and marine carbon cycle. But, before that another quick check of $\delta^{13}C$ implementation could be done. I support publication of the manuscript once the comments below have been taken into account.

We would like to thank reviewer #1 for their feedback on our manuscript. We have considered all of the comments carefully and addressed them in turn below, with our responses in blue-italics.

We are confident that our implementation is mathematically correct and that there are no bugs in the code because we have already completed extensive checks, including:

- *Verifying that our equations are balanced, and that no carbon (^{12}C or ^{13}C) is being created or destroyed.*
- *Running with $\delta^{13}C_{atm}$ equal to 0 ‰ and no isotopic fractionation effects (all α values set to 1.0). In this simulation, the $\delta^{13}C_{DIC}$ values remained constant at 0 ‰.*
- *Running with $\delta^{13}C_{atm}$ equal to -6.5 ‰ and no isotopic effects (all α values set to 1.0). In this simulation, the $\delta^{13}C_{DIC}$ equilibrated at -6.5 ‰.*

P3, L. 5-8 and table 1: the carbon isotopes enabled model LOVECLIM is missing from this list, with references Mouchet, 2013 (Radiocarbon) and Menviel et al., 2015 (GBC), as the carbon cycle models and carbon isotopes implementation are different in iLOVECLIM and LOVECLIM.

Our intention was to provide illustrative examples of ^{13}C-enabled models across a range of complexities as opposed to a complete list of all ^{13}C-enabled models, but we are happy to add this additional example in the revised manuscript.

P3, L9-11: This sentence has to be amended. The list of carbon isotopes enabled models on L. 8 includes 2-dimensional, 3-dimensional models, OGCMs and AOGCMs; and apart from 3 there are OGCMs with similar resolution as the model described here. It thus cannot be suggested that all these models are too simple to study abrupt climate changes, moreover when the model presented in this study probably provides similar performances/capability to some models in that list (even more so because it focuses on ocean processes, and because in this model "sea ice formation and melt do not affect salinity distributions", p5, L. 16).

FAMOUS is a full-complexity, ocean-atmosphere General Circulation Model (AOGCM). Even though it does not have the high resolution of the more complex models that are cited (e.g. PISCES and CESM), for simulations of coupled ocean-atmosphere interactions, and particularly when atmospheric variability is important, FAMOUS is an improved model compared to the Earth System Models of Intermediate Complexity Models (that do not have a full-primitive equation atmosphere or that have more limited vertical resolution in the atmosphere) and the ocean-only models. However, these are specific cases and we agree that the highlighted sentence makes a crude point that is not well justified. We will therefore remove the sentence from the revised manuscript.

P5, L. 14: suggest to replace “EEP”, by “equatorial Pacific” as simulated primary production is higher both in the western and eastern Pacific. Please also modify the end of the sentence as follows: “attributed to excessive upwelling in the EEP”.

We will revise this sentence to “However, primary production is higher than observed in the equatorial Pacific, which is attributed to excessive upwelling in the eastern equatorial Pacific (Palmer and Totterdell, 2001)”.

From P10, L. 28 to p11, L.2: I would suggest to be really cautious here and eventually add a few words/sentences of explanation as it is stated that $\delta^{13}C$ is high in the Southern Ocean because of CO_2 outgassing, and high in the EEP because AABW is upwelled. This is of course only true in this experiment where no biological fractionation is taken into account. If all processes are taken into account AABW would have a low $\delta^{13}C$. Therefore, to account for the quick reader, it might be best to repeat “because there is no biological fractionation in this experiment”. In addition, I doubt that “AABW” is upwelled in the EEP. It is sufficient to simply state that the upwelled water has a high $\delta^{13}C$ value because it is mostly southern-sourced waters. But, it is quite surprising to see such high values in the EEP in no-bio-fract. In addition, the model $\delta^{13}C$ is globally too high in std. The authors investigate thoroughly the impact of fractionation during photosynthesis, but could it be a problem linked to gas-exchange parametrization? Is the right hand side of Equation 5 really needed? Would plotting $\delta^{13}C$ vs PO_4 in the model help in confirming that everything is correct?

We will revise the manuscript as suggested:

“When both the equilibrium and kinetic fractionation effects are included during air-sea gas exchange (no-bio-fract), the large-scale $\delta^{13}C_{DIC}$ distributions are closely related to the SST patterns because of the temperature dependence of $\alpha_{aq\leftarrow g}$ and $\alpha_{DIC\leftarrow g}$ (Figure 4b). In the absence of biological fractionation, relatively high $\delta^{13}C_{DIC}$ values (> +2.5 ‰) are simulated in the Southern Ocean due to the combined effect of CO_2 outgassing and low SSTs, both of which cause ^{13}C enrichment. The $\delta^{13}C_{DIC}$ values in the Arctic Ocean are comparably low because the model has more extensive sea ice in the Northern Hemisphere than in the Southern Hemisphere, which inhibits air-sea gas exchange. The highest values (+3.00 ‰) are simulated in the eastern equatorial Pacific where there are high rates of net CO_2 outgassing and southern-sourced waters, which have a high $\delta^{13}C_{DIC}$ signature in this simulation because there is no biological fractionation, are upwelled.”

The right hand side of the equation 5 is necessary because we are carrying the tracer as a ratio ($^{13}C/^{12}C$). Please see the derivation in Appendix B.

Plotting the simulated $\delta^{13}C$ values against the corresponding PO_4^{3-} values, which we have derived using Redfield ratios because FAMOUS only contains a single nitrogenous nutrient, suggests that everything is correct. The model captures the expected relationship between the two variables, with approximately a -1 ‰ change in $\delta^{13}C$ per 1 μmol kg^{-1} change in PO_4^{3-} (Figure R1).

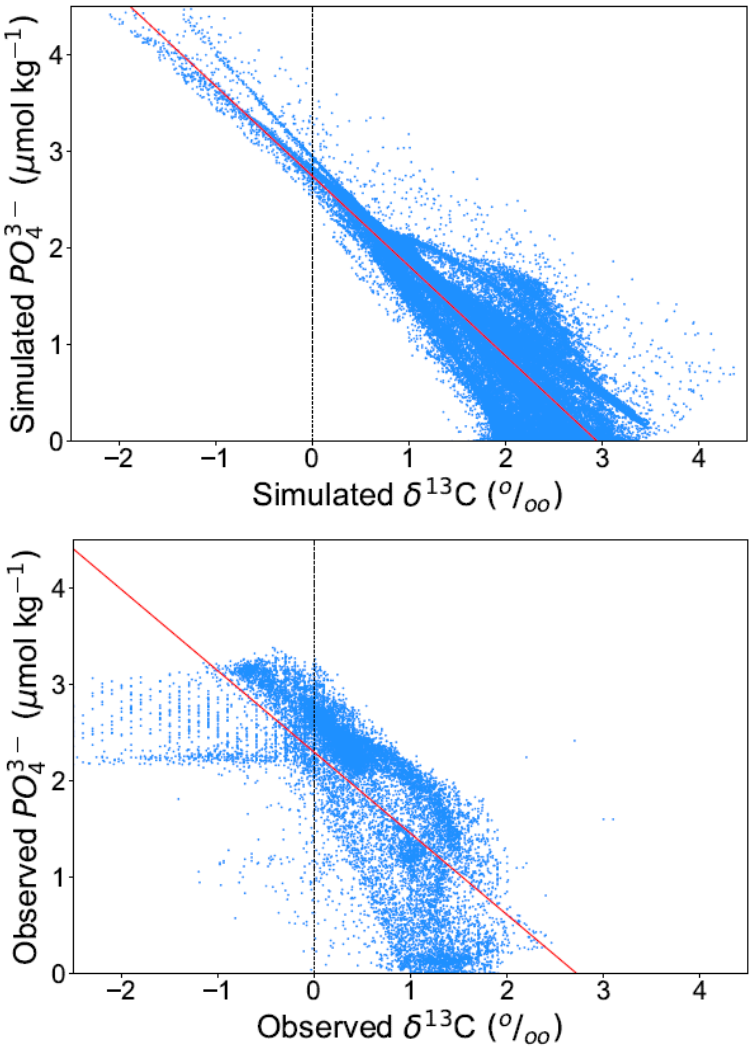

Figure R1: *$\delta^{13}C$ versus PO_4^{3-} during the 1990s in the std simulation (top) and in the GLODAPv.2 data set (bottom). The red lines are the linear regression lines for each set of data.*

Figure 6 is quite helpful. The profiles are a bit surprising, but are discussed in details and compared with Schmittner et al. 2013. Note that the Bern3D and LOVECLIM profiles are also shown in Menviel et al., 2015, and could help in assessing the accuracy of the latitudinal d13C distributions. *Menviel et al. (2015) conducted a different set of sensitivity experiments to those presented by us (section 3.1) and Schmittner et al. (2013). Instead, they conducted a suite of experiments with freshwater forcing in the North Atlantic and Southern Oceans, and changes in the wind stress. Thus, whilst interesting, their results are not comparable to ours.*

Since our original manuscript submission, we have accessed the raw data for the four equivalent simulations conducted by Schmittner et al. (2013), which we discuss in section 3.1. We have therefore added these lines on to Figure 5 and Figure 6 so that readers can make a direct comparison between the two models. The figures and the corresponding captions will therefore be revised as follows:

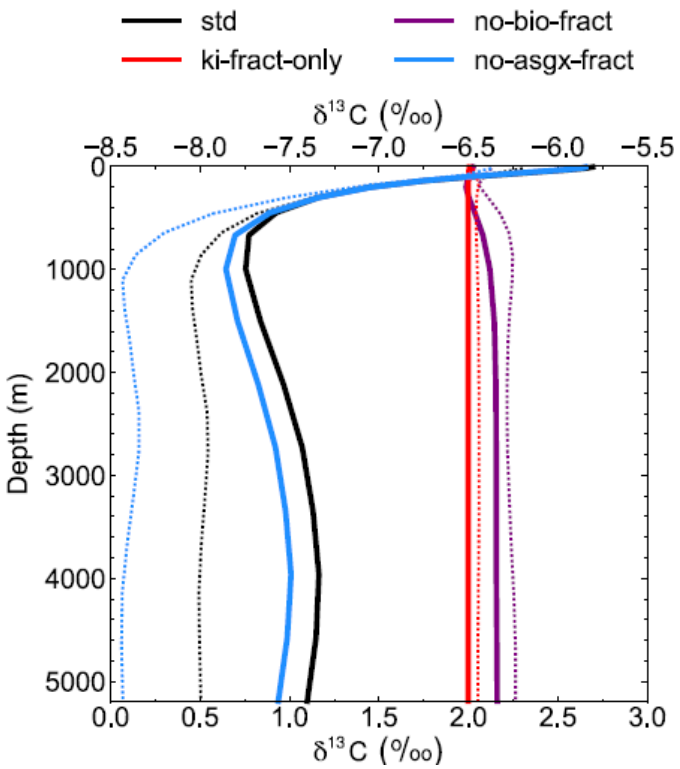

Figure 5: *Depth profiles of globally averaged $\delta^{13}C_{DIC}$ at the end of the sensitivity experiment spin-up simulations (years 9900 to 10,000). The std (black) and no-bio-fract (purple) simulations use the bottom axis, whilst the ki-fract-only (red) and no-asgx-fract (blue) simulations use the top axis. The dotted lines are the equivalent simulations conducted by Schmittner et al. (2013) with the UVic ESM: std (black) and no-bio (purple) on the bottom axis; ki-only (red) and const-gasx (blue) on the top axis.*

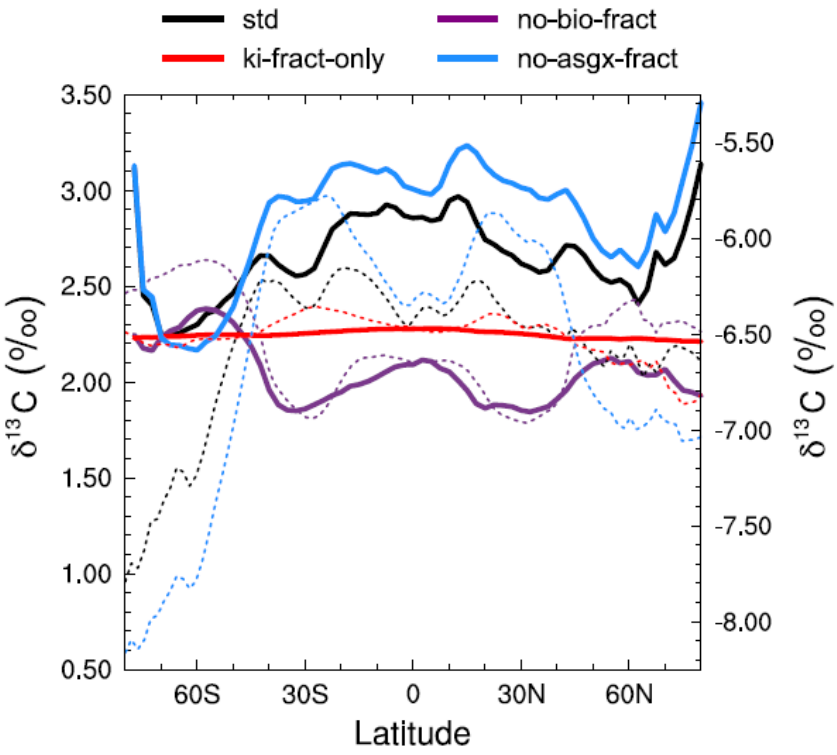

Figure 6: *Zonally averaged mean annual surface $\delta^{13}C_{DIC}$ at the end of the sensitivity experiment spin-up simulations (years 9900 to 10,000). The std (black) and no-bio-fract (purple) simulations use the left-hand axis, whilst the ki-fract-only (red) and no-asgx-fract (blue) simulations use the right-hand axis. The dotted lines are the equivalent simulations conducted by Schmittner et al. (2013) with the UVic ESM: std (black) and no-bio (purple) on the left-hand axis; ki-only (red) and const-gasx (blue) on the right-hand axis.*

Figure 3: Why is $CaCO_3$ in grey? Since there is no fractionation during $CaCO_3$ formation, then maybe the line from DIC to $CaCO_3$ should be black. There should be an arrow going from DIC to atm. "Atmosphere" should in fact be "Atm CO_2".

- *$CaCO_3$ is in grey because the export of $CaCO_3$ in FAMOUS is represented as an instantaneous redistribution of alkalinity and carbon at depth (i.e. the model doesn't actually carry $CaCO_3$ as a tracer). This will be clarified in the revised figure caption.*
- *The $CaCO_3$ formation line was red because, in reality, this process is affected by isotopic fractionation and, in the model, is coded to allow for constant isotopic fractionation. In all of our simulations, we have chosen to set α_{CaCO3} equal to 1.0 because we found that including isotopic fractionation during $CaCO_3$ formation has a negligible effect on the $\delta^{13}C_{DIC}$ values (as discussed in section 2.2). For clarity, we will revise the figure so that this arrow is orange, and amend the caption to clarify that the orange arrow represents a process that can include a constant isotopic fractionation effect (should future users of the code wish to so), but that this effect has not been included in any of the simulations presented in our manuscript.*
- *We will revise the figure with an arrow going from the DIC pool to the atmospheric pool, but will make it clear in the revised figure caption that the atmosphere doesn't see the outgassed isotopic ratio because atmospheric $\delta^{13}C$ is prescribed.*
- *We will alter "Atmosphere" to "Atmospheric CO_2" to be more accurate.*

The figure and the corresponding caption will therefore be revised as follows:

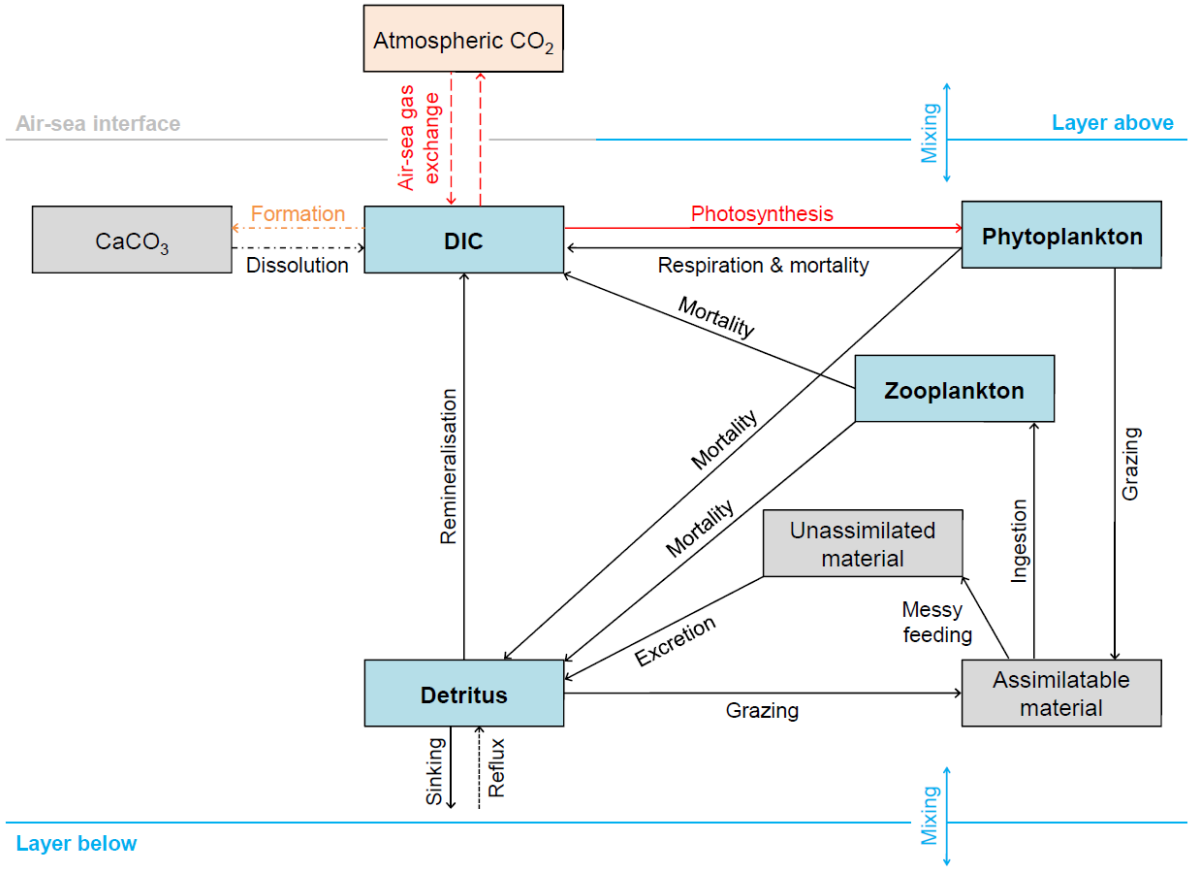

Figure 2: *Schematic overview of the ^{13}C implementation in FAMOUS. Blue boxes represent permanent carbon pools. Grey boxes represent temporary carbon pools (note that $CaCO_3$ is a temporary carbon pool because the export of $CaCO_3$ in FAMOUS is represented as an instantaneous redistribution of alkalinity and carbon at depth). The orange box represents the prescribed atmospheric carbon pool. The dashed lines represent fluxes of $^{13}C/^{12}C$. However, note that the outgassed $^{13}C/^{12}C$ has no effect on $\delta^{13}C_{atm}$ because FAMOUS does not currently have a fully interactive carbon cycle. Solid lines represent fluxes of ^{13}C. Dot-dashed lines represent processes that occur below the lysocline (≈ 2500 m below sea level). The dotted line represents the reflux of detrital material from the seafloor to the surface layer. Red lines represent fractionation effects. The orange line represents isotopic fractionation during calcium carbonate formation (α_{CaCO3}), which is included in the code as a user-specified constant. Note that all simulations presented in this study were run without fractionation during calcium carbonate formation (i.e. α_{CaCO3} = 1.0, which is equivalent to a fractionation effect of 0 ‰).*

Figure 7: The authors might consider modifying this figure as it looks like 3 times the same plot. I understand that it might be the point, but maybe best to move some (L95, L97) to SI. The choice of the colorbars could be revised: it is hard (impossible) to see any feature in a), and difficult in the right hand side panels. Are experiments L95 and L97 described in the methods? It would be helpful to also include them in Table 2

- *We will move the original Figure 7 into the supplementary material and replace it in the main manuscript with a 4-panel plot containing the observed values, the std simulation corrected for the mean surface bias, the std simulation, and the difference between the std and observed values:*

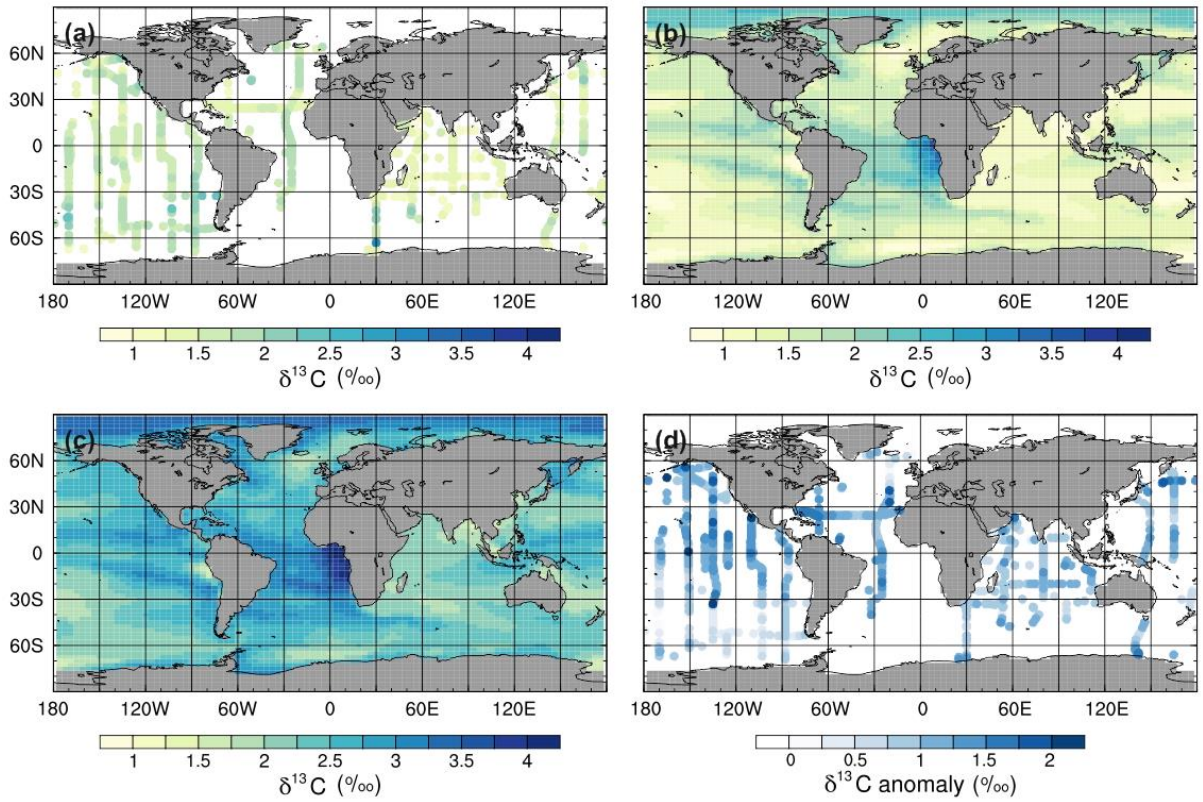

Figure 7: *Mean annual surface $\delta^{13}C_{DIC}$ during the 1990s: (a) observations from GLODAPv2 (Key et al., 2015; Olsen et al., 2016), (b) the std simulation corrected for the mean surface bias (0.97 ‰), which is calculated as ∑(simulated-observed)/number of observations, (c) the std simulation, and (d) std minus GLODAPv2.*

- *We do not have the same difficulty in seeing the features in the subplots. Perhaps the issue is with the low resolution conversion of the figure in the supplied file. We are therefore attaching a PDF of the figure to this response, which is the resolution that will be supplied for the final manuscript. In this version, the colour scale displays the features clearly. We prefer not to change the colour scheme because we selected it very carefully: it is colour-blind friendly and the colour gradations are easy to interpret. We are not aware of an alternative colour scheme that would improve the visualisation of these data.*
- *Yes, experiments L95 and L97 are described in the methods (see lines 18 to 27 on page 8, and lines 9 to 13 on page 10 of the original manuscript). We will add these simulations to Table 2 for completeness.*

Table 2: Overview of the fractionation factors used in the sensitivity experiments.

Simulation	α_k	$\alpha_{aq\leftarrow g}$, $\alpha_{DIC\leftarrow g}$	α_p
std	Standard[1]	Variable[2]	Variable – $\alpha_{POC\leftarrow aq}$ calculated as per Eq. (**Error! Reference source not found.**)
ki–fract-only	Standard	1	1
no-asgx-fract	1	1	Variable – $\alpha_{POC\leftarrow aq}$ calculated as per Eq. (**Error! Reference source not found.**)
no-bio-fract	Standard	Variable	1
L95	Standard	Variable	Variable – $\alpha_{POC\leftarrow aq}$ calculated as per Eq. (10)
L97	Standard	Variable	Variable – $\alpha_{POC\leftarrow aq}$ calculated as per Eq. (11)

[1] 0.99919

[2] Calculated as per Eq. (**Error! Reference source not found.** – **Error! Reference source not found.**)